Bulk Properties of Transition Metals: A Challenge for the Design of Universal Density Functionals

Patanachai Janthon,[1,2,3] Sijie (Andy) Luo,[4] Sergey M. Kozlov,[1]
Francesc Viñes,[1] Jumras Limtrakul,[2,3] Donald G. Truhlar,[4] and Francesc Illas[1*]

[1]*Departament de Química Física & Institut de Química Teòrica i Computacional (IQTCUB), Universitat de Barcelona, c/Martí i Franquès 1, 08028, Barcelona, Spain*

[2]*Department of Chemistry and NANOTEC Center for Nanoscale Materials Design for Green Nanotechnology, Kasetsart University, Bangkok 10900, Thailand*

[3]*PTT Group Frontier Research Center, PTT Public Company Limited, 555 Vibhavadi Rangsit Road, Chatuchak, Bangkok 10900, Thailand*

[4]*Department of Chemistry, Chemical Theory Center, and Supercomputing Institute, University of Minnesota, Minneapolis, Minnesota 55455-0431, USA*

Abstract

Systematic evaluation of the accuracy of exchange-correlation functionals is essential to guide scientists in their choice of optimal method for a given problem when using density functional theory. In this work accuracy of one Generalized Gradient Approximation (GGA) functional, three meta-GGA functionals, one Non-separable Gradient Approximation (NGA) functional, one meta-NGA, and three hybrid GGA functionals was evaluated for calculations of closest interatomic distances, cohesive energies, and bulk moduli of all 3*d*, 4*d*, and 5*d* bulk transition metals that have face centered cubic (*fcc*), hexagonal closed packed (*hcp*), or body centered cubic (*bcc*) structures (a total of 27 cases). Our results show that including the extra elements of kinetic energy density and Hartree-Fock exchange energy density into gradient approximation density functionals does not usually improve them. Nevertheless, the accuracies of the Tao-Perdew-Staroverov-Scuseria (TPSS) and M06-L meta-GGAs and the MN12-L meta-NGA approach the accuracy of the PBE GGA, so usage of these functionals may be advisable for systems containing both solid-state transition metals and molecular species. The N12 NGA functional is also shown to be almost as accurate as PBE for bulk transition metals, and thus it could be a good choice for studies of catalysis given its proven good performance for molecular species.

1. Introduction

Kohn-Sham Density Functional Theory (KS-DFT) has become a workhorse for treating complex problems in both the gaseous and condensed phases. The accuracy of KS-DFT rests entirely on the accuracy of one's approximation to the exchange-correlation (xc) functional. Functional development has considered a wide range of application targets. In particular, there are numerous validation studies for atoms and molecules, many more than for condensed-phase quantum chemistry and solid-state physics. A particularly important area that still needs further study, aside from its importance for studying heterogeneous catalysis and electrochemistry,[1] is the accuracy of available xc functionals for transition metal solids.

One route to improve xc functionals is to add more elements, which takes one to a higher rung on the Jacob's ladder[2] of xc functionals. The first rung is the local Spin Density Approximation (LSDA), which depends on only local spin densities. Including dependences only on spin densities and their gradients yields gradient approximations, such as the Generalized Gradient Approximation[3,4] (GGA) or Non-separable Gradient Approximation[5] (NGA), which constitute the second rung; further addition of kinetic energy density leads to meta functionals, such as meta-GGAs and meta-NGAs, which form the third rung, and, finally, including Hartree-Fock (HF) exchange leads to hybrid functionals, in particular hybrid gradient approximations and hybrid meta approximations, which form the fourth rung. Through the third rung, the exchange-correlation energy density depends only on local variables, but hybrid functionals are nonlocal.

One tentative conclusion about xc functionals that has been advanced is that adding elements from third and fourth rungs has not lead to better performance for metals,[6,7] and various studies have been carried out with gradient approximations that provide further experience related to this issue.[7-9] Furthermore, although hybrid functionals are justifiably the most popular kind of functionals in molecular chemistry [10] (because of their good performance), for extended systems they have increased computational demands as compared to local functionals due to the long range of the exchange in real space programs and to the requirement for dense Brillouin zone sampling in plane wave programs.[11] Hybrid functionals also have the disadvantage of bringing in HF static correlation error, which is important for many molecular and solid-state transition metal compounds[8,12,13] In fact, when one tries to estimate the optimal percentage of HF exchange in a hybrid functional suitable

for transition metal solids, the resulting fraction is close to zero,[14,15] leading to the conclusion that the inclusion of HF exchange is detrimental for the accuracy of xc functionals for solid transition metals. Therefore, the inadequacy of hybrid functionals in the description of transition metals is to be expected.[16]

As a result of both the above kinds of issues —performance and cost— local functionals have remained the most popular choice for solid-state transition metal investigations even though hybrid functionals by construction reduce self-interaction error. A similar situation pertains even when the choice of xc functionals is restricted to local ones, where, even although meta functionals also have the potential to reduce self-interaction error,[17] gradient approximations have been preferred to meta functionals partly for the greater simplicity of popular GGAs, but also because meta functionals have not always seemed to significantly improve the accuracy. However this situation seems unsatisfactory because both hybrid functionals and meta functionals have better performance than GGAs on molecules composed of atoms lighter than the transition metals.[18-21] Thus, there is a strong interest in certain fields, such as heterogeneous catalysis, nanotechnology, and materials chemistry, to use meta or hybrid functionals because these research lines often deal with the interaction between transition metal surfaces and light main-group compounds. Meta and hybrid functionals also yield more accurate band gaps,[15,22-25] which may be important for metal-oxide systems that are ubiquitous as supports in catalysis, photocatalysis, and nanotechnology. In light of these practical considerations, there is a need for a more systematic investigation of accuracy of meta and hybrid functionals for various properties of transition metal solids.

In this article we assess the accuracy of several meta and hybrid functionals for bulk transition metals. Namely, we consider shortest interatomic distances, δ, cohesive energies, E_{coh}, and bulk moduli, B_0, of all 27 bulk transition metals that have face centered cubic (*fcc*), hexagonal closed packed (*hcp*), or body centered cubic (*bcc*) structures. We present new results for the following functionals:

- GGA: SOGGA11[26]
- NGA: N12[5]
- meta-GGAs: Tao-Perdew-Staroverov-Scuseria (TPSS),[27] revised Tao-Perdew-Staroverov-Scuseria (revTPSS),[28] and meta M06-L[29]

- meta-NGA: MN12-L[30]
- hybrid gradient approximations: Perdew-Burke-Ernzerhof (PBE0), [31] Heyd-Scuseria-Ernzerhof (HSE06),[32] and Lee-Yan-Parr B3LYP[33]

We compare the new results obtained here to the results obtained previously[34] with PBE, a GGA functional that performed best in a previous study of two LSDA functionals: the Perdew-Zunger functional (PZ81)[35] based on Ceperley-Alder (CA) numerical results[36] and Vosko-Wilk-Nusair (VWN, usually denoted also as VWN5), [37] and four gradient approximations: PBE,[38] PBEsol,[39] RPBE,[40] and PW91.[41] Note that PW91 performance was found to be close to that of PBE.

2. Computational Details

The computational procedures were kept as close as possible to those used in a previous work by Janthon *et al*.[34] Calculations were performed using a locally modified version of Vienna Ab Initio Simulation Package VASP.[42] The atomic cores were described by the Projector Augmented Wave (PAW) method,[43] using the potentials recommended in the documentation (see supporting information for full specification) which take account of kinetic energy density dependencies when present. An optimized Monkhorst−Pack[44] k-points grid of 7×7×7 was used in all bulk calculations, which was found to be sufficient for accurate total energy calculations with the smallest unit cell. A kinetic energy cutoff of 415 eV for the plane-wave basis set was employed throughout, guaranteeing variations of total energy below 1 meV with respect to bigger basis sets.

Scalar relativistic effects in the core region are included in the PAW potentials. Previous calculations have shown that relativistic effects on the valence electrons of heavy transition metals lead to negligible deviations from this standard PAW approximation, i.e., interatomic distances changes ranging 0.002−0.005 Å and differences in bulk moduli of 3−5 GPa.[45]

The electronic structure calculations were not spin polarized, with the exception of the calculations on the ferromagnetic Fe, Ni, and Co bulk systems and on isolated metal atoms. Note by passing that magnetic moments, yet not being the topic of discussion, nicely agree with experimental values. Compare for instance PBE values of X.X, X.X, and X.X μ_B with experimental values of 2.2, 1.7, and 0.6 μ_B for Fe, Co, and Ni, respectively.[46] Moreover, present results reveal, in accordance with previous calculations, the antiferromagnetic bulk

structure of Cr, with a magnetic moment of X.X as obtained at PBE level, similar to the previously reported value of 0.92 μ_B obtained at PW91 level.[47] [FV: Modify depending on the data, also include comment for TPSS and HSE06] Optimizations were performed using the tetrahedron smearing method of Blöchl *et al*.[48] with an energy width of 0.2 eV to speed up convergence with the final energies extrapolated to zero smearing. In bulk calculations, ionic positions and cell volumes were optimized using the conjugate gradient algorithm until pressures and total energies were converged within 0.01 GPa and 10 meV, respectively. The isolated atoms were placed in a large unit cell with broken symmetry of 9×10×11 Å dimensions to ensure proper occupancy of degenerate orbitals and thus obtain properly defined atomic energies. When needed orbital occupancy was imposed to match that of the isolated atom; further details concerning atomic configuration and energies are found in a previous article.[34] The large unit cell allows one to sufficiently suppress spurious interactions between periodic images (< 1 meV). In this case calculations were carried out at the **Γ** point in reciprocal space.

Shortest interatomic distances within a crystal cell, δ, depend on the lattice parameter *a*. For the *fcc* structures δ equals $a/\sqrt{2}$, while for *bcc* it equals $\sqrt{3}/2$. In the case of *hcp*, δ depends on lattice paratemers *a* and *c*; and δ may equal *a* or $(c^2/4+a^2/3)$ depending on the c/a ratio.

Cohesive energies, E_{coh}, were expressed as an energy difference per atom as follows:

$$E_{coh} = E_{at} - \frac{E_{bulk}}{N}$$

where E_{at} is the energy of the isolated metal atom in a vacuum, and E_{bulk} is the energy of the bulk unit cell containing *N* atoms. With this definition, the larger the positive values of cohesive energies, the stronger is the chemical bonding within the solid.

The bulk modulus, B_0, is defined as

$$B_0 = -V_0\left(\frac{\partial P}{\partial V}\right)_{T,Vo}$$

where *V* is the volume of the solid, *P* is an external pressure, and the negative sign is used because the volume decreases when a positive external pressure is applied. Bulk modulus is obtained as the slope of linear regression of P versus V using the volumes at equilibrium geometry and at geometries with ±0.05 and ±0.10 Å variations of the lattice constants. One

has to keep in mind that another more accurate procedure is the adjustment of energy points to a Murnaghan equation of state,[49] which can provide slightly. In fact, bulk moduli obtained at PBE level with a similar calculation setup, but through the adjustment to Murnaghan equation, are ~5 GPa lower than presently calcualted.[11] However, the direct calculation approximation is expected to have very little effect for our comparative purposes.

In this present work, we consider the 27 transition metals that exhibit close-packed structures, which may display *fcc*, *hcp*, or *bcc* structures. We specifically exclude La and solid Hg, that have hexagonal and rhombohedral unit cells, respectively, and Mn, which has a cubic unit cell containing 58 atoms, although it is similar to a *bcc* structure. The reason for these exclusions is that preliminary work showed that metals exhibiting these non-close-packed structures can exhibit different trends than the typical metals, and specialized consideration is required to do them justice.

In the following, as the previous work,[34] in addition to cohesive energy and bulk modulus, the shortest interatomic distance within a crystal cell, δ, will be compared to the experimental values. We present results for individual metals, and to more clearly see some trends, we also present mean errors, in particular Mean Signed Error (MSE), Mean Absolute Error (MAE), and mean absolute percentage error (MAPE).

3. Comparison between Experimental and Theoretical Results

To compare calculated results to the available experimental data in a reasonable fashion, we must take account of experimental variability and the differences between the measurements and the calculations. First of all, significant differences can be found between experimental values reported for cohesive energies and bulk moduli in different sources, and on average, different entries in the Crystallographic Open Database[50] yield shortest interatomic distances with variations of ~0.05 Å. Among many entries in the database we selected most recent ones, as was done previously.[34] For cohesive energies and bulk moduli, we picked experimental values from the handbook by Young.[51] However, in a recent study by Lejaeghere *et al.*[52] assessing the performance of the PBE functional for almost all elemental solids in the periodic table, alternative sets of experimental values are used, mostly from Kittel or Villars and Daams.[53,54] See Tables S2-S4 in Supporting Information for more details. With some exceptions the experimental values used in the present work compare nicely to the values used in Lejaeghere *et al.*, with median discrepancies for δ, E_{coh}, and B_0

being 0.004 Å, 0.06 eV, and 5 GPa, respectively. If we used the same set of experimental values as in Ref. 52, the reported MAPE would change by less than 0.5% for δ, 0.25% for E_{coh}, and 2% for B_0, and such changes have a negligible effect on our conclusions.

The second type of complication comes from the fact that experiments are typically performed at room temperature, whereas the calculations reported here reflect the internal energies at minima of potential energy surfaces. Results measured at room temperature differ from the calculated values mainly by inclusion of zero-point phonon energy and thermal phonon energy. Rather than account for these effects in each computation, reverse corrections are applied to the experimental values. Here, we apply the same corrections as in Lejaeghere *et al.*,[52] which decrease δ by 0.003–0.022 Å, increase E_{coh} by 0.01–0.06 eV, and increase B_0 by 1–17 GPa. In general, these corrections move experimental values closer to calculated ones, typically decreasing average MAPEs by 0.04%, 0.2%, and 2% for δ, Ecoh and B0, respectively. For a clearer comparison with other studies, we list both corrected and uncorrected experimental values, but only corrected ones were used calculate errors and draw conclusions.

4. Results and Discussion

4.1. Interatomic Distances

KS-DFT is generally well suited to predict interatomic distances accurately. In most of the cases studied here, accuracy is rather high. Table 1 shows ~1% discrepancies between the calculated and the experimental data. One can compare present results with previous computational studies carried out for a reduced set of metals. Indeed, present PBE results nicely correlate with previous calculations on Cu, Rh, Pd, and Ag fcc metals, with deviations below 0.01 Å.[11] Another suitable comparison with a previous study with over a dozen *fcc* and *bcc* transition metals revealed lattice parameters deviations of ~ 0.03 Å for PBE functional, and below 0.02 Å for TPSS functional,[55] corroborating the precision of present calculations. Surprisingly, the most accurate xc functionals for interatomic distances are HSE06 and PBE0, which both slightly overestimate δ on average. Nevertheless, all considered functionals underestimate interatomic distances of the lightest transition metals, Sc, Ti, V, and Cr, with the exception of HSE06 for Sc. Curiously present calculations reveal a nice match of HSE06 for Cr interatomic distances, in discrepancy with a previous study

highlighting a high overestimation of the functional (23%) for bulk Cr.[56] Moreover, interatomic distances of magnetic Fe, Co, and Ni are nicely described by hybrid functionals. Calculated and experimental lattice parameters are found in Table S8 of Supplementary Materials.

The accuracy of all meta functionals is noticeably lower for δ of Zn, Cd, and Re. The least accurate results, among the eight functionals considered here, are obtained by the SOGGA11 and B3LYP functionals. Upon a careful inspection of the present values and previous data,[34] one could conclude that B3LYP is even less accurate than LSDA functionals for structural data of bulk transition metals. Finally, despite satisfactory overall performance, MN12-L yields poor results for Sc and Fe.

The performance of revTPSS is not superior to that of TPSS. The reason may be that revTPSS is based on PBEsol, which was parameterized to predict better lattice constants of solid state materials, while TPSS is based on more versatile PBE. However, for solid transition metals the performance of PBEsol is worse than that of PBE (even for interatomic distances),[34] and so is the performance of revTPSS compared to the accuracy of TPSS. In fact, revTPSS tends to be more accurate than TPSS only for heavy and late transition metals, i.e. from Zr to Cd (except Tc and Ru) and from Re to Au.

The table does show some correlation between accuracy of the functional and the type of crystal structure. For example, M06-L and the hybrid functionals are somewhat less accurate for *fcc* metals with absolute errors 0.01-0.02 Å higher than average, see Tables S5-S7 in Supporting Information for more details. At the same time PBE0 and HSE06 are more accurate for *hcp* metals (MAE of only 0.014 to 0.016 Å, respectively), while M06-L, TPSS, revTPSS, and B3LYP are more accurate for *bcc* metals with absolute errors lower by 0.016–0.025 Å than average.

4.2. Cohesive Energies

Cohesive energies are generally harder to predict correctly than interatomic distances; and Table 2 shows that many functionals are systematically biased towards overestimation or underestimation of the energies. For example, in most of the cases, the considered hybrid functionals strongly underestimate E_{coh} by ~1 to 1.8 eV, which renders them the least accurate functionals for this quantity (B3LYP is even less accurate than LSDA). This is a result to be expected due to the poor description of transition metals by hybrid functionals,[16]

here critically affecting the cohesive energies. The most accurate results come from PBE, TPSS, and N12 (MAEs of ~0.35 eV), followed by revTPSS and SOGGA11 (MAEs of 0.52 eV and 0.54 eV).

As for interatomic distances, there are certain materials for which all meta functionals show lower accuracy. Cohesive energies of Ni, Co, and Fe are overestimated by 0.75 – 2 eV (except MN12-L for Co). M06-L and MN12-L also overestimate E_{coh} of Cu, Sc, and Ti. The correlation between the functional accuracy and the crystal structure is rather weak in this case, but we find that MN12-L is quite accurate for *bcc* metals (MAE of 0.35 eV), while PBE0 and HSE06 are particularly bad for them (MSE of ~-1.4 eV).

4.3. Bulk Moduli

Bulk moduli are also quite hard to calculate correctly, and almost all the considered meta and hybrid functionals (except B3LYP) overestimate them, as shown in Table 3. The most accurate results are produced by PBE, followed by TPSS, while the least accurate functionals for this property are MN12-L and revTPSS.

All considered functionals significantly overestimate the bulk moduli of V, Ni, Re, and especially Cr. Also all meta functionals show lower accuracy for B_0 of Cu and Zn. The PBE and HSE06 hybrid functionals, in general, have an accuracy similar to that of meta functionals, but their performance is less satisfactory for Tc, Ru, and heavy transition metals from W to Ir.

Bulk moduli exhibit a strong correlation of functional accuracy with the crystal structure. For example, MN12-L, TPSS, revTPSS, PBE0, and HSE06 suffer a 60-70% increase in MAPE for the metals with *bcc* crystal structure. M06-L and B3LYP have lower accuracy for *fcc* metals (by 60 and 90%, respectively), but are somewhat more accurate for *hcp* metals (by 40 and 65%, respectively). Finally, PBE0 is 35% more accurate for B0 of *fcc* metals, whilst HSE06 is 30% better for transition metals with *hcp* structure.

4.4. Overall Performance

Average discrepancies between theoretical and corrected experimental values are listed in Table 4 (for comparison with uncorrected experimental values see Tables S2-S4 and for particular metals and properties see Figure S1 and Tables S5-S7 in Supporting

Information). For the sake of better presentation MAPE values are also displayed on Figure 1.

Table 4 shows the best performance for PBE gradient approximation and the TPSS meta functional, with HSE06, N12, M06-L, and PBE0 performing moderately well, and revTPSS, B3LYP, SOGGA11, and MN12-L performing worst. TPSS is slightly more accurate than PBE for cohesive energies, while it tends to significantly overestimate bulk moduli. Both PBE and TPSS MAPE values are in line with previous calculations with a restricted set of transition metals.[55] As expected TPSS corrects the tendency of PBE to overestimate interatomic distances by eliminating the diverging exchange potential at the nuclei.[21] The use of TPSS may be favorable when molecular systems are also to be considered in the same study.[21] Nevertheless, when one is only interested in the accurate prediction of lattice parameters, hybrid functionals such as PBE0 or HSE06 may be preferred. In fact, HSE06 always shows performance slightly better than that of PBE0, which may reflect the higher suitability of Hartree-Fock exchange restricted only to short range for treatment of solid-state systems, although it may also result from cancellation of errors.

On the other hand, if one is mainly interested in accurate energetics, then the N12 gradient approximation is a good choice, especially when one considers its good performance for both cohesive energies and molecular species. The poor performance of the hybrid functionals considered here for the cohesive energies of bulk transition metals may be related to a poorer description of the gas-phase atoms used as energy references.[11] However, this does not explain the mediocre accuracy of the bulk moduli calculations with PBE0, HSE06, and B3LYP.

Although no solid-state data was used in designing M06-L, whereas solid-state data was used for designing MN12-L, it is interesting that M06-L shows better performance in the present tests. Note by passing that M06-L was found to properly describe cumbersome CO adsorption on Pt(111), which strengthens its usefulness even in complex systems.[57] B3LYP turns out to be the least accurate hybrid functional of those studied here for transition metal solids. In most of the cases it overestimates interatomic distances and underestimates cohesive energies, being even less accurate than LSDA. Earlier this poor performance was explained by the LYP correlation functional not satisfying the homogeneous electron gas limit and the HF exchange issue.[58,59]

5. Conclusions

The accuracy of selected meta and hybrid functionals for solid transition metals has been assessed by comparing calculated interatomic distances, cohesive energies, and bulk moduli to experimental values. We assess the accuracy based on the set of 27 bulk transition metals having *fcc*, *hcp*, or *bcc* structures. For proper comparison the measured values were corrected for finite temperature and zero-point vibrations as in Lejaeghere *et al.*[52] The obtained results are also compared to those from a previous study by Janthon *et al.*,[34] where the performance of LSDA and GGA functionals was assessed in a very similar manner.

Table 5 presents average discrepancies between theory and experiment averaged over members of a given functional type: Gradient Approximations (GA), meta functionals, and hybrid functionals. The present results show that meta and hybrid functionals present, on average, no improvement in accuracy over gradient approximation functionals for transition metal solids. TPSS is found to be the most accurate among meta exchange-correlation functionals, but even it essentially matches accuracy of PBE for interatomic distances and cohesive energies, while being somewhat less accurate for bulk moduli. M06-L was found to be moderately accurate as well. Given that N12, TPSS, M06-L, and MN12-L functionals are more accurate for molecular systems than PBE, one could foresee their successful application to processes involving both solid state metals and molecular species, e.g. those in surface science, heterogeneous catalysis, etc. Hybrid functionals (except B3LYP, maybe due to the uniform gas limit violation[58]) were found to be the most accurate methods for calculations of interatomic distances in bulk transition metals. However, the performance of all considered hybrid functionals for cohesive energies is disappointing, and their accuracy for the bulk moduli is just moderate, as expected from the known problematic of HF exchange static correlation error, critical for the description of transition metals.[16]

6. Supporting Information

Table S1 provides details of the pseudopotentials used in the calculations. Tables S2-S4 display experimental list of interatomic distances, cohesive energies, and bulk moduli (un)corrected for ZPE and finite-temperature values, as well as differences from the two sources. Tables S5-S7 are analogous to Table 4 but considering only *fcc*, *bcc*, or *hcp* metals. Table S8 is analogous to Table 1 but displaying lattice constants. Figure S1 sketches the most accurate functional(s) from those studied in the description of interatomic distances, cohesive energies, and bulk moduli across the transition metals.

7. Acknowledgments

This work was supported by the Spanish *Ministerio* grants (FIS2008-02238, CTQ2012-30751) and *Generalitat de Catalunya* grants (2009SGR1041 and XRQTC) and, in part, by grants from the National Science and Technology Development Agency (NSTDA Chair Professor and NANOTEC Center for the Design of Nanoscale Materials for Green Nanotechnology), the Kasetsart University Research and Development Institute (KURDI), the Commission on Higher Education, Ministry of Education ("the National Research University Project of Thailand (NRU)" and "Postgraduate Education and Research Programs in Petroleum and Petrochemicals and Advanced Materials"). P. J. would like to thank the Office of the Higher Education Commission, Thailand for supporting him with a grant under the program Strategic Scholarships for Frontier Research Network for the PhD Program Thai Doctoral degree and the Graduate School of Kasetsart University for his research. S.M.K. thanks the *Spanish Ministerio de Educacion* for a pre-doctoral grant AP2009-3379. F.V. thanks the Spanish MICINN for the postdoctoral grants under the programs *Juan de la Cierva* and *Ramón y Cajal* (JCI-2010-06372 and RYC-2012-10129) and F.I. acknowledges additional support through the ICREA Academia award for excellence in research. This work was also supporting in part by the Air Force Office of Scientific Research under grant number FA9550-11-1-0078.

Table 1. Calculated and experimental shortest interatomic distances (δ, in Å) for bulk transition metals.

		GGA		NGA	Meta-GGA			Meta-NGA	Hybrid			exp.	exp. corr.[b]
	CS	PBE	SOGGA11	N12	TPSS	revTPSS	M06-L	MN12-L	PBE0	HSE06	B3LYP		
Sc	*hcp*	3.214	3.066	3.194	3.198	3.192	3.149	3.013	3.238	3.252	3.230	3.254	3.244
Ti	*hcp*	2.884	2.806	2.864	2.862	2.855	2.859	2.850	2.862	2.865	2.883	2.897	2.889
V	*bcc*	2.577	2.561	2.582	2.559	2.554	2.581	2.559	2.548	2.548	2.573	2.613	2.606
Cr	*bcc*	2.459	2.479	2.467	2.442	2.435	2.457	2.428	2.429	2.428	2.457	2.498	2.485
Fe	*bcc*	2.453	2.498	2.457	2.431	2.424	2.484	2.598	2.502	2.522	2.517	2.460	2.450
Co	*hcp*	2.470	2.496	2.438	2.444	2.438	2.472	2.489	2.452	2.482	2.498	2.497	2.488
Ni	*fcc*	2.489	2.506	2.455	2.453	2.443	2.419	2.370	2.471	2.480	2.510	2.493	2.484
Cu	*fcc*	2.567	2.502	2.551	2.517	2.499	2.476	2.485	2.563	2.564	2.606	2.556	2.544
Zn	*hcp*	2.644	2.522	2.465	2.522	2.465	2.490	255.2	2.638	2.640	2.781	2.665	2.645
Y	*hcp*	3.543	3.419	3.511	3.522	3.518	3.562	3.615	3.554	3.559	3.565	3.556	3.548
Zr	*hcp*	3.197	3.144	3.166	3.179	3.171	3.218	3.195	3.187	3.185	3.213	3.179	3.174
Nb	*bcc*	2.873	2.882	2.871	2.862	2.852	2.888	2.871	2.860	2.857	2.888	2.859	2.854
Mo	*bcc*	2.749	2.716	2.692	2.734	2.729	2.748	2.726	2.724	2.721	2.755	2.725	2.721
Tc	*hcp*	2.722	2.707	2.685	2.700	2.689	2.706	2.689	2.679	2.677	2.717	2.710	2.705
Ru	*hcp*	2.658	2.643	2.627	2.637	2.624	2.649	2.623	2.608	2.610	2.649	2.650	2.642
Rh	*fcc*	2.717	2.695	2.683	2.689	2.674	2.702	2.676	2.674	2.672	2.723	2.539	2.532
Pd	*fcc*	2.794	2.756	2.766	2.761	2.742	2.794	2.755	2.768	2.765	2.827	2.753	2.745
Ag	*fcc*	2.941	2.861	2.901	2.890	2.867	2.940	2.899	2.924	2.925	2.992	2.889	2.877
Cd	*hcp*	2.990	2.954	2.913	2.920	2.880	2.883	3.002	2.964	2.971	3.139	2.979	2.959
Hf	*bcc*	2.875	3.067	2.854	2.857	2.844	2.886	2.839	2.864	2.861	2.886	3.131	3.126
Ta	*bcc*	2.751	2.875	2.746	2.736	2.724	2.744	2.718	2.725	2.724	2.761	2.860	2.856
W	*hcp*	2.751	2.761	2.746	2.736	2.724	2.744	2.718	2.725	2.724	2.761	2.741	2.738
Re	*hcp*	2.755	2.756	2.723	2.742	2.730	2.742	2.724	2.721	2.720	2.759	2.567	2.562
Os	*fcc*	2.694	2.700	2.673	2.685	2.673	2.688	2.656	2.660	2.661	2.698	2.675	2.671
Ir	*fcc*	2.741	2.747	2.712	2.727	2.710	2.733	2.705	2.712	2.711	2.759	2.715	2.710
Pt	*fcc*	2.811	2.809	2.780	2.789	2.769	2.806	2.771	2.778	2.777	2.835	2.772	2.766
Au	*hcp*	2.950	2.921	2.912	2.912	2.888	2.945	2.913	2.922	2.919	2.992	2.879	2.870

[b] ZPE and finite temperature corrections to experimental values adapted from Lejaeghere *et al.*[52]

Table 2. Calculated and experimental cohesive energies (E_{coh}, in eV/atom) of bulk transition metals.[a]

		GGA		NGA	Meta-GGA			Meta-NGA	Hybrid			exp.	exp. corr.[b]
	CS	PBE	SOGGA11	N12	TPSS	revTPSS	M06-L	MN12-L	PBE0	HSE06	B3LYP		
Sc	*hcp*	4.12	3.63	4.53	4.21	4.28	5.77	5.32	3.42	3.52	2.76	3.90	3.93
Ti	*hcp*	5.45	5.37	5.78	5.47	5.52	6.40	6.85	4.00	4.08	3.35	4.84	4.88
V	*bcc*	6.03	5.12	5.77	5.73	5.94	6.30	5.75	3.40	3.48	3.25	5.30	5.34
Cr	*bcc*	4.00	4.37	4.21	4.21	4.44	4.55	4.33	1.54	1.57	1.57	4.09	4.15
Fe	*bcc*	4.87	4.96	4.65	5.23	5.48	5.39	5.13	3.22	3.29	2.81	4.28	4.32
Co	*hcp*	5.27	4.28	5.32	6.21	6.51	5.66	4.54	3.24	3.31	2.86	4.43	4.47
Ni	*fcc*	4.87	4.11	4.96	5.40	5.24	5.75	6.15	3.19	3.26	2.85	4.44	4.48
Cu	*fcc*	3.48	3.32	3.36	3.73	4.06	4.39	4.42	3.01	3.06	2.54	3.48	3.51
Zn	*hcp*	1.12	0.86	1.14	1.34	1.59	1.67	1.58	1.12	1.17	0.44	1.35	1.38
Y	*hcp*	4.13	4.56	4.59	4.23	4.38	4.96	5.78	3.74	3.85	3.00	4.39	4.42
Zr	*hcp*	6.16	7.43	6.73	6.30	6.50	6.75	5.15	5.60	5.70	4.69	6.29	6.32
Nb	*bcc*	6.98	7.86	7.23	7.20	7.42	8.02	7.40	5.96	6.12	5.59	7.44	7.47
Mo	*bcc*	6.21	6.95	6.89	6.59	6.91	6.90	6.82	5.10	5.19	4.82	6.80	6.84
Tc	*hcp*	6.85	8.52	7.34	7.18	7.58	7.15	7.04	5.41	5.54	4.90	7.13	7.17
Ru	*hcp*	6.67	8.00	7.21	7.10	7.52	6.76	6.79	5.06	5.21	4.56	6.74	6.80
Rh	*fcc*	5.62	7.00	6.00	6.22	6.61	6.12	6.33	4.39	4.54	3.92	5.72	5.76
Pd	*fcc*	3.71	4.54	3.55	4.01	4.40	4.24	4.70	2.85	2.96	2.43	3.90	3.93
Ag	*fcc*	2.49	3.20	2.49	2.73	3.04	3.28	3.60	2.28	2.35	1.87	2.94	2.96
Cd	*hcp*	0.73	1.72	0.76	0.96	1.21	1.37	1.06	0.78	0.85	0.18	1.16	1.18
Hf	*bcc*	6.40	7.61	6.84	6.53	6.78	7.32	5.78	6.04	6.12	5.02	6.42	6.44
Ta	*bcc*	8.27	8.45	8.26	8.51	8.84	8.99	7.58	7.63	7.74	6.58	8.09	8.11
W	*hcp*	9.07	9.16	9.02	8.81	9.19	9.86	8.43	7.76	7.79	7.29	8.79	8.83
Re	*hcp*	7.82	7.97	7.89	8.25	8.68	7.97	9.45	6.75	6.85	5.89	8.02	8.06
Os	*fcc*	8.29	8.72	7.84	8.46	8.80	8.32	9.46	7.20	7.34	6.24	8.17	8.22
Ir	*fcc*	7.32	8.31	7.74	7.71	8.21	7.03	7.35	6.19	6.36	5.28	6.92	6.96
Pt	*fcc*	5.50	6.58	5.71	5.79	6.25	5.97	6.17	4.69	4.83	3.99	5.85	5.87
Au	*hcp*	2.99	3.86	3.03	3.28	3.62	3.61	3.79	2.80	2.88	2.23	3.81	3.83

[a] See footnotes to Table 1.

Table 3. Calculated and experimental bulk moduli (B_0, in GPa) of bulk transition metals.[a]

		GGA	Meta-GGA			Meta-NGA	Hybrid			exp.	exp. corr.
	CS	PBE	TPSS	revTPSS	M06-L	MN12-L	PBE0	HSE06	B3LYP		
Sc	*hcp*	55.0	59.4	57.9	71.6	82.5	57.2	56.2	51.4	54.6	55.6
Ti	*hcp*	113.5	119.1	122.6	129.4	125.4	132.4	125.2	120.0	106.0	108.3
V	*bcc*	183.1	198.9	212.0	193.3	199.1	225.9	214.9	199.1	155.0	158.9
Cr	*bcc*	261.2	274.4	293.3	268.6	298.4	290.7	291.8	271.8	160.0	174.5
Fe	*bcc*	195.3	218.5	232.8	169.8	77.2	165.1	176.7	151.1	163.0	169.8
Co	*hcp*	212.5	236.3	244.2	236.4	172.7	222.4	203.5	204.1	186.0	193.0
Ni	*fcc*	193.9	226.4	239.6	262.9	323.2	226.3	216.4	169.4	179.0	185.5
Cu	*fcc*	146.9	184.3	198.7	183.4	181.5	135.2	133.8	113.4	133.0	140.3
Zn	*hcp*	78.4	106.4	124.9	109.2	92.0	88.0	76.5	62.8	64.8	69.7
Y	*hcp*	40.7	44.4	42.1	47.0	34.5	39.9	41.5	42.5	41.0	41.7
Zr	*hcp*	95.5	98.3	98.7	96.9	96.3	88.0	99.0	94.4	94.9	95.9
Nb	*bcc*	171.1	178.9	190.6	170.4	179.2	190.6	183.7	176.7	169.0	172.0
Mo	*bcc*	261.3	278.2	285.3	262.9	286.8	288.4	295.7	262.8	261.0	264.7
Tc	*hcp*	307.6	324.1	336.5	307.2	333.3	357.2	355.4	310.2	297.0	303.1
Ru	*hcp*	308.2	334.8	347.6	312.5	349.5	366.3	361.9	314.1	303.0	317.7
Rh	*fcc*	256.4	282.8	298.5	258.8	287.6	294.0	284.7	241.2	282.0	288.7
Pd	*fcc*	169.4	192.1	207.9	153.3	181.4	176.0	163.3	138.8	189.0	195.4
Ag	*fcc*	83.3	110.2	120.9	93.6	98.3	89.9	83.6	71.2	98.8	103.8
Cd	*hcp*	49.6	61.1	68.0	64.1	37.9	58.1	55.3	38.9	49.8	53.8
Hf	*bcc*	108	112.6	115.4	116.2	114.8	112.3	115.7	111.7	108.0	109.7
Ta	*bcc*	195.3	205.9	212.6	201.2	210.5	217.4	205.8	193.3	191.0	193.7
W	*hcp*	316.2	329.8	335.7	320.1	348.2	347.0	356.4	315.9	308.0	312.3
Re	*hcp*	372.1	393.1	407.1	402.2	396.7	428.7	424.8	376.9	360.0	368.8
Os	*fcc*	402.6	426.4	449.9	427.7	482.4	460.9	460.9	396.9	418.0	424.6
Ir	*fcc*	347.3	367.0	391.8	339.6	396.9	397.1	392.8	328.1	358.0	365.2
Pt	*fcc*	250.9	272.6	290.2	250.7	273.9	278.1	275.6	225.4	277.0	284.2
Au	*hcp*	138.4	162.7	174.9	140.3	143.4	141.2	146.6	112.0	166.0	174.8

[a] See footnotes to Table 1.

Table 4. Statistical analysis of differences between the experimental results extrapolated to 0 K and corrected for zero-point vibrations[a] and the calculated values: interatomic distances (δ, in Å), cohesive energies (E_{coh}, in eV/atom) and bulk modulus (B_0, in GPa). MAPE values are given in percent.

		GGA		NGA	Meta-GGA			Meta-NGA	Hybrid		
		PBE	SOGGA11	N12	TPSS	revTPSS	M06-L	MN12-L	PBE0	HSE06	B3LYP
δ	MSE	0.03	0.00	-0.02	0.00	-0.01	0.01	0.00	0.01	0.01	0.05
	MAE	0.04	0.05	0.05	0.04	0.04	0.05	0.05	0.03	0.03	0.06
	MAPE	1.4	1.9	1.8	1.4	1.5	1.9	2.0	1.2	1.1	2.2
	rank	3	7	6	3	5	7	9	2	**1**	10
E_{coh}	MSE	-0.04	0.40	0.12	0.21	0.50	0.46	0.40	-1.08	-0.99	-1.66
	MAE	0.34	0.52	0.36	0.35	0.52	0.49	0.64	1.08	0.99	1.66
	MAPE	10.9	11.4	8.6	10.0	11.2	10.6	13.7	24.0	21.7	37.7
	rank	4	6	**1**	2	5	3	7	9	8	10
B_0	MSE	-0.4	—	—	17.5	28.7	9.8	17.7	20.3	17.5	-8.6
	MAE	15.1	—	—	20.0	28.7	23.4	32.4	27.2	24.9	22.4
	MAPE	8.4	—	—	12.7	17.6	15.4	19.6	14.2	12.2	12.9
	rank	**1**	—	—	3	7	6	8	5	2	4
average rank		2.7	6.5	3.5	2.7	5.7	5.3	8.0	5.3	3.7	8.0

Table 5. Statistical analysis of differences between the experimental results as in Table grouping functionals by type.

		GA[a]	Meta[b]	Hybrid[c]
δ (Å)	MSE	0.00	0.00	0.03
	MAE	0.05	0.05	0.04
	MAPE	1.7	1.7	1.5
E_{coh} (eV/atom)	MSE	0.16	0.39	-1.24
	MAE	0.42	0.50	1.24
	MAPE	10.3	11.4	27.8
B_0 (GPa)	MSE	-0.4	18.4	9.7
	MAE	15.1	26.1	24.8
	MAPE	8.4	16.3	13.1

[a] averaged over PBE, N12, and SOGGA11

[b] averaged over TPSS, revTPSS, M06-L, and MN12-L

[c] averaged over PBE0, HSE06, and B3LYP

Figure 1. Mean Absolute Percentage Errors (MAPE) for the interatomic distances, δ; cohesive energies, E_{coh}; and bulk moduli, B_0, of 27 transition metals with respect to experimental values extrapolated to 0 K and corrected for zero-point vibrations. MAPE of δ has been multiplied by a factor of 10 for a better presentation. Data for LDA xc functionals, PBE, PW91, PBEsol, and RPBE is adapted from Janthon *et al*.[34]

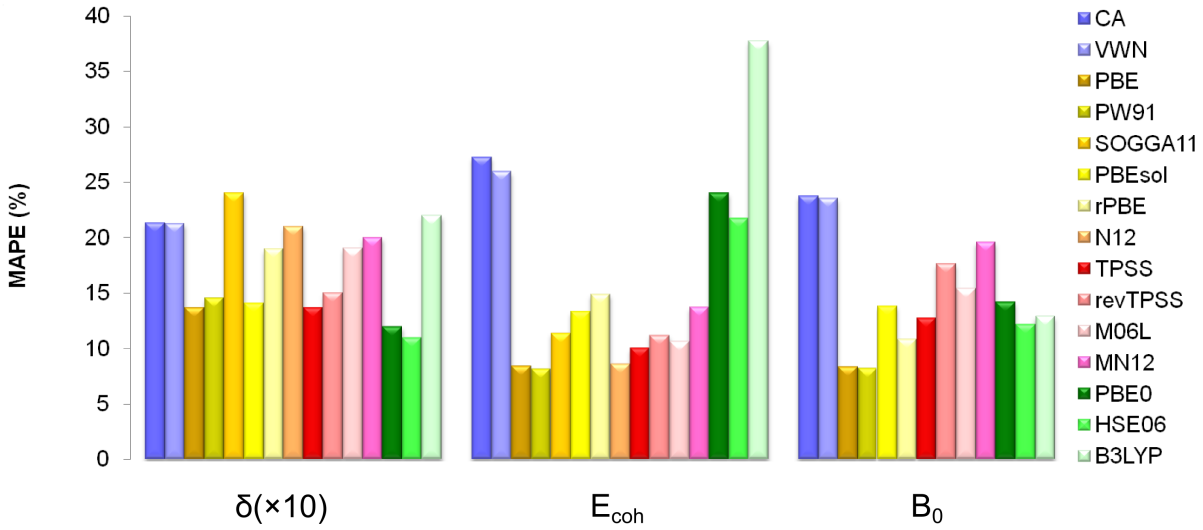

References

(1) Cramer, C. J.; Truhlar, D. G. *Phys. Chem. Chem. Phys.* **2009**, *11*, 10757.

(2) Perdew, J. P.; Schmidt, K. *AIP Conf. Proc.* **2001**, *577*, 1.

(3) Langreth, D. D.; Mehl, M. J. *Phys. Rev. B* **1983**, *28*, 1809.

(4) Perdew, J. P.; Wang, Y. *Phys. Rev. B* **1986**, *33*, 8800.

(5) Peverati, R.; Truhlar, D. G. *J. Chem. Theory Comput.* **2012**, *8*, 2310.

(6) Schultz, N. E.; Zhao, Y.; Truhlar, D. G. *J. Chem. Phys.* **2006**, *124*, 224105.

(7) Schultz, N. E.; Zhao, Y.; Truhlar, D. G. *J. Phys. Chem. A* **2005**, *109*, 11127.

(8) Harvey, J. N. *Annu. Rep. Prog. Chem., Sect. C* **2006**, *102*, 203.

(9) Schultz, N. E.; Zhao, Y.; Truhlar, D. G. *J. Phys. Chem. A* **2005**, *109*, 4388.

(10) Sousa, S. F.; Fernandes, P. A.; Ramos, M. J. *J. Phys. Chem. A* **2007**, *111*, 10439.

(11) Paier, J.; Marsman, M.; Hummer, K.; Kresse, G.; Gerber, I. C.; Ángyán, J. G. *J. Chem. Phys.* **2006**, *124*, 154709.

(12) Polo, V.; Kraka, E.; Cremer, D. *Mol. Phys.* **2002**, *100*, 1771.

(13) Grafenstein, J.; Kraka, E.; Cremer, D. *Phys. Chem. Chem. Phys.* **2004**, *6*, 1096.

(14) Perdew, J. P.; Ernzerhof, M.; Burke, K. *J. Chem. Phys.* **1996**, *105*, 9982.

(15) Marques, M. A. L.; Vidal, J.; Oliveira, M. J. T.; Reining, L.; Botti, S. *Phys. Rev. B* **2011**, *83*, 035119.

(16) Ashcroft, N. W.; Mermin, N. D.; *Solid State Physics*; Saunders College Publishing, Orlando, FL, 1976; p 335.

(17) Becke, A. D. *J. Chem. Phys.* **1998**, *109*, 2092.

(18) Staroverov, V. N.; Scuseria, G. E.; Tao, J.; Perdew, J. P. *J. Chem. Phys.* **2003**, *119*, 12129.

(19) Mardirossian, N.; Parkhill, J. A.; Head-Gordon, M. *Phys. Chem. Chem. Phys.* **2011**, *13*, 19325.

(20) Peverati, R.; Truhlar, D. G. *Phys. Chem. Chem. Phys.* **2012**, *14*, 13171.

(21) Peverati R.; Truhlar, D. G. *Phil. Trans. Roy. Soc. A* **2014**, *372*, 20120476.

(22) Muscat, J.; Wander, A.; Harrison, N. M. *Chem. Phys. Lett.* **2001**, *342*, 397.

(23) Tomić, S.; Montanari, B.; Harrison, N. M. *Phys. E* **2008**, *40*, 2125.

(24) Zhao Y.; Truhlar, D. G. *J. Chem. Phys.* **2009**, *130*, 074103.

(25) Peverati, R.; Truhlar, D. G. *J. Chem. Phys.* **2012**, *136*, 134704.

(26) Peverati, R.; Zhao, Y.; Truhlar, D. G.; *J. Phys. Chem. Lett.* **2011**, *2*, 1991.

(27) Tao, J.; Perdew, J. P.; Staroverov, V. N.; Scuseria, G. E. **2003**, *91*, 146401.

(28) Perdew, J. P.; Ruzsinszky, A.; Csonka, G. I.; Constantin, L. A.; Sun, J. *Phys. Rev. Lett.* **2009**, *103*, 026403.

(29) Zhao, Y.; Truhlar, D. G. *J. Chem. Phys.* **2006**, *125*, 194101.

(30) Peverati, R.; Truhlar, D. G. *Phys. Chem. Chem. Phys.* **2012**, *14*, 13171.

(31) Adamo, C.; Barone, V. *J. Chem. Phys.* **1999**, *110*, 6158.
(32) Krukau, A. V.; Vydrov, O. A.; Izmaylov, A. F.; Scuseria, G. E. *J. Chem. Phys.* **2006**, *125*, 224106.
(33) Becke, A. D. *J. Chem. Phys.* **1993**, *98*, 5648.
(34) Janthon, P.; Kozlov, S. M.; Viñes, F.; Limtrakul, J.; Illas, F. *J. Chem. Theory Comput.* **2013**, *9*, 1631.
(35) Perdew, J. P.; Zunger, A. *Phys. Rev. B* **1981**, *23*, 5048.
(36) Ceperley, D. M.; Alder, B. J. *Phys. Rev. Lett.* **1980**, *45*, 566.
(37) Vosko, S. H.; Wilk, L.; Nusair, M. *Can. J. Phys.* **1980**, *58*, 1200.
(38) Perdew, J. P.; Burke, K.; Ernzerhof, M. *Phys. Rev. Lett.* **1996**, *77*, 3865.
(39) Perdew, J. P.; Ruzsinszky, A.; Csonka, G. I.; Vydrov, O. A.; Scuseria, G. E.; Constantin, L. A.; Zhou, X.; Burke, K. *Phys. Rev. Lett.* **2008**, *100*, 136406
(40) Hammer, B.; Hansen, L. B.; Nørskov, J. K. *Phys. Rev. B* **1999**, *59*, 7413.
(41) Perdew, J. P.; Wang, Y. *Phys. Rev. B* **1992**, *45*, 13244.
(42) Kresse, G.; Furthmüller, J. *Phys. Rev. B* **1996**, *54*, 11169.
(43) Blöchl, P. E. *Phys. Rev. B* **1994**, *50*, 17953.
(44) Monkhorst, H. J.; Pack, J. D. *Phys. Rev. B* **1976**, *13*, 5188.
(45) Grabowski, B.; Hickel, T.; Neugebauer, J. *Phys. Rev. B* **2007**, *76*, 024309.
(46) Billas, I. M. L.; Châtelain, A.; de Heer, W. A. *Science* **1994**, *265*, 1682.
(47) Hafner, R.; Spišák, D.; Lorenz, R.; Hafner, J. *Phys. Rev. B* **2002**, *65*, 184432.
(48) Blöchl, P. E.; Jepsen, O.; Andersen, O. K. *Phys. Rev. B* **1994**, *49*, 16223.
(49) Murnaghan, F.D. *Proc. Natl. Acad. Sci.* **1944**, *30*, 244.
(50) Gražulis, S.; Chateigner, D.; Downs, R. T.; Yokochi, A. T.; Quiros, M.; Lutterotti, L.; Manakova, E.; Butkus, J.; Moeck, P.; Le Bail, A. J. *Appl. Crystallogr.* **2009**, *42*, 726.
(51) Young, D. A. *Phase Diagrams of the Elements*; University of California Press: Berkeley, CA, 1991; p 273.
(52) Lejaeghere, K.; Van Speybroeck, V.; Van Oost, G.; Cottenier, S. *Crit. Rev. Solid State Mater. Sci.* **2014**, *39*, 1.
(53) Kittel, C. *Introduction to Solid State Physics*; John Wiley & Sons, Inc, 8th ed., 2005; p 20.
(54) Villars P.; Daams, J. *J. Alloys Compd.* **1993**, *197*, 177.
(55) Haas, P.; Tran, F.; Blaha, P. *Phys. Rev. B* **2009**, *79*, 085104.
(56) Chevrier, V. L.; Ong, S. P.; Armiento, R.; Chan, M. K. Y.; Ceder, G. *Phys. Rev. B* **2010**, *82*, 075122.
(57) Luo, S.; Zhao, Y.; Truhlar, D. G. *J. Phys. Chem. Lett.* **2012**, *3*, 2975.
(58) Kurth, S.; Perdew, J.P.; Blaha, P. *Int. J. Quantum Chem.* **1999**, *75*, 889.
(59) Paier, J.; Marsman, M.; Kresse, G. *J. Chem. Phys.* **2007**, *127*, 024103.

Graphic for TOC